

# Atomic structure and electronic properties of the GaN/ZnO (0001) interface

J. VON PEZOLD, P. D. BRISTOWE

*Department of Materials Science and Metallurgy, University of Cambridge, Pembroke Street, Cambridge CB2 3QZ, UK*

The stability and electronic structure of cation- and anion-compensated interfaces between (0001) lattice-matched slabs of GaN and ZnO have been considered. It was found that, irrespective of interfacial polarity, cation-compensated interfaces are by approximately 20 meV/unit cell more stable than the corresponding anion-compensated interfaces. Valence band offsets of 1.0 and 0.5 eV have been found at the cation- and anion-compensated interfaces, respectively. © 2005 Springer Science + Business Media, Inc.

## 1. Introduction

Due to its favourable electronic properties GaN has been investigated extensively over the last 10 years. In particular its large, direct band gap has been exploited for the fabrication of optoelectronic devices, such as short-wavelength LEDs [1] and LDs [2]. Despite the substantial successes achieved so far, there are still a number of issues that need to be resolved to realise the full potential of GaN-based devices. In particular, its high melting temperature in excess of 2500 K precludes the large-scale growth of bulk GaN, which is why the material is generally grown epitaxially. Sapphire and SiC are commonly used as substrates. However, due to their significant lattice constant and thermal expansion coefficient mismatches with GaN, the GaN epilayers grown on them tend to be highly defective. Many different materials have been tried, but so far no ideal substrate has been found.

In many ways ZnO is very similar to GaN. It is also a semiconductor material with the wurtzite structure and has similar lattice constants (basal-plane lattice constant difference of only 1.8%). In addition, ZnO exhibits an equally large band gap of 3.37 eV at room temperature [3], is strongly bonded like GaN with bond energies as large as 1.89 eV [4] and displays a correspondingly high melting point of 2248 K [5]. It is therefore not surprising that ZnO has also been considered for short-wavelength device applications. However, its isomorphism with GaN, the closely matching lattice constants as well as its similar thermal expansion coefficient make ZnO a promising candidate as a buffer layer or indeed substrate (bulk samples of ZnO recently became available at relatively low cost [6]). Its isomorphism, in particular, sets it apart from other substrates that have been considered previously and should reduce the density of threading defects [7] extending into the GaN epilayers. This hypothesis has been corroborated somewhat by Hamdani *et al.* [8], who have reported the absence of the generally observed yellow luminescence band in the PL spectrum of GaN epilayers grown on high quality ZnO substrates.

The epitaxial growth of high quality GaN films on ZnO (0001) buffer layers has also been reported by various other groups [9–13]. However, there are some important problems associated with the use of ZnO as a substrate for GaN epitaxy. In particular, ZnO is attacked at high temperatures in reducing atmospheres and is therefore ill suited for growth under conditions typically employed in MOCVD or HVPE [14]. Therefore low temperature techniques such as MBE or PLD are generally used. The problem is further relieved by using a low temperature GaN buffer layer between the ZnO substrate and the epitaxial GaN film, which has been found to effectively protect the ZnO substrate [11]. Another pertinent issue is the observation [15] that GaN films grown on the Zn-face of ZnO are unstable against Ga-droplet formation. However, Hamdani *et al.* [11], who have studied the growth of GaN on both faces of ZnO, do not report the formation of Ga droplets on the Zn-face of the ZnO substrate. Instead, they observed that the GaN epilayer grown on the Zn-face exhibited a considerably rougher surface than the GaN epilayer grown on the O-face ZnO surface. It is also worth mentioning that GaN has been successfully used as a buffer layer for ZnO heteroepitaxy [5, 16–18].

In addition to the similar structural and thermal properties of GaN and ZnO, there is also an interest in the electronic properties of the GaN/ZnO (0001) interface. In particular, the heterovalent nature of the interface potentially allows for band-offset engineering, as will be explained below. Recently the formation of *n*-ZnO/*p*-GaN heterojunction light-emitting diodes has been reported [19, 20]. However, despite the considerable technological potential of the GaN/ZnO (0001) heterointerface, its fundamental properties are only poorly understood. In particular the relative stabilities of the different possible interfacial atomic structures, which determine the observed band-offset of 0.8 eV at the interface [28], have not been considered so far. The only theoretical study available is one by Nakayama and Murayama [21], who have reported an average value for the band offset at the interface, without considering the stability

of the different interfacial atomic configurations. It is therefore the aim of this study to determine the relative stability of the different interfaces and to derive the corresponding band offsets. The two materials are artificially lattice matched by using an averaged basal-plane lattice constant of the bulk GaN and ZnO structures in all calculations reported. The effects of strain are currently being investigated and will be reported in a separate communication.

## 2. Theoretical method

### 2.1. Atomic mixing at the GaN/ZnO (0001) heterovalent interface

In bulk wurtzite materials, such as GaN and ZnO, each atom forms four bonds to its next nearest neighbours. Each cation-anion pair contains eight valence electrons that are equally distributed amongst its four bonds. Hence each bond is occupied by two electrons. In other words, each atom donates  $1/4$  of its valency to each of its four bonds. Hence the occupation of a bond between atoms A and B is given by

$$f_{\text{occ}}^b = (Z_v^A + Z_v^B)/4 \quad (1)$$

where  $f_{\text{occ}}^b$  is the occupation of the bonds formed by cation A and anion B, as determined by their respective valency  $Z_v^A$  and  $Z_v^B$ . At the (0001) interface, bonds between atoms are formed, whose valencies do not add up to eight and hence the bond occupation  $f_{\text{occ}}^b$  is different from two. Thus for the Zn–N interface each Zn–N bond will be electron deficient by  $1/4$  of an electron, while bonds in the Ga–O interface will contain an electron excess of  $1/4$  of an electron. Hence electronic charge will accumulate at the Ga–O interface, while the Zn–N interface will be electron deficient, which results in the

formation of a negatively and a positively charged interface, respectively. The charged interfaces would give rise to electric fields that extend throughout the overlayer, which is energetically unfavourable, as was first pointed out by Harrison *et al.* [22]. The accumulation of charges can only be avoided if the number of electron-deficient bonds in the interface is balanced by the same number of electron-rich bonds. Due to the polarity of the semiconductor materials under consideration, this balance can only be achieved by allowing atomic mixing of the interfacial layers. Taking the Ga–O interface between the Ga-polar GaN slab and the O-polar ZnO slab as an example, the charge accumulation can either be compensated by replacing  $1/4$  of all the Ga atoms in the interfacial Ga layer by Zn atoms, or alternatively by replacing  $1/4$  of all the O atoms in the interfacial O layer by N atoms, as is shown in Fig. 1. It should be noted that there are other possible compensations, such as interfaces with two mixed layers; however, these have been disregarded in this study.

### 2.2. Formation energies and chemical potentials

In order to compare the stability of the various interfaces, the interfacial formation energy,  $E_f^{\text{int}}$  is used, which is generally defined as [23]:

$$E_f^{\text{int}} = \frac{1}{2} \left( E^{\text{tot}} - \sum_A n^A \mu^A \right) / (ab) \quad (2)$$

A = Ga, N, Zn, O

where  $E^{\text{tot}}$  is the calculated total energy of the supercell containing the interface,  $n^A$  is the number of atoms of species A and  $\mu^A$  is the chemical potential of atom A.  $(ab)$  corresponds to the number of atoms in the layers

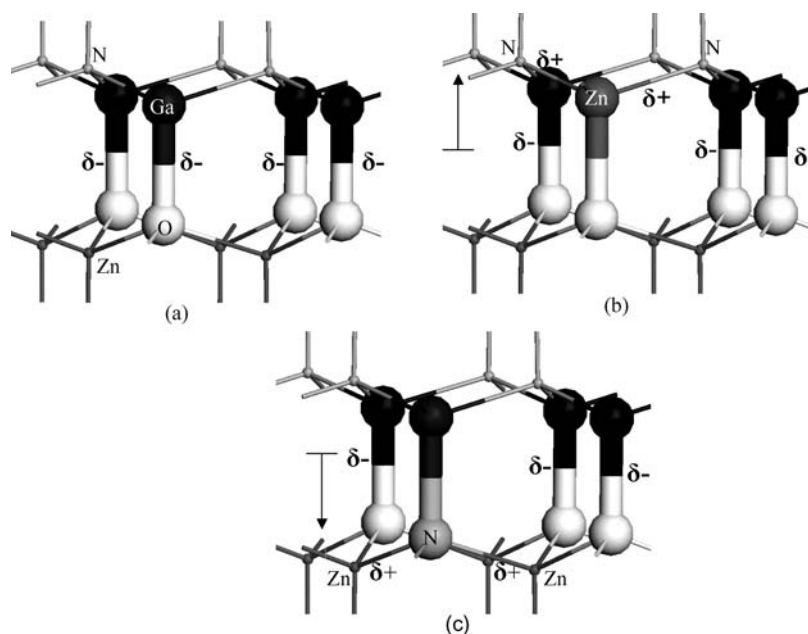


Figure 1 (a) Abrupt (non-compensated), (b) cation-compensated and (c) anion-compensated Ga–O interface. The charge accumulation can only be avoided if the total number of electron rich Ga–O bonds is balanced by the same number of electron-deficient Zn–N bonds. Cation- and anion-compensated interfaces give rise to interfacial dipoles pointing in opposite directions, as indicated by the black arrows; Note the colour scheme: Ga atoms are black, N atoms are light grey, Zn atoms are dark grey and O atoms are white.

parallel to the interface. Thus the interface formation energy refers to the  $(1 \times 1)$  cell. The prefactor of  $1/2$  accounts for the fact that the supercells actually consist of two interfaces which are assumed to be identical.

In thermodynamic equilibrium the chemical potentials are in equilibrium with the bulk, i.e.

$$\begin{aligned}\mu^{\text{GaN}} &= \mu^{\text{Ga}} + \mu^{\text{N}} \\ \mu^{\text{ZnO}} &= \mu^{\text{Zn}} + \mu^{\text{O}}\end{aligned}\quad (3)$$

where  $\mu^{\text{GaN}}$  is the chemical potential of bulk GaN and  $\mu^{\text{ZnO}}$  is the chemical potential of bulk ZnO. Hence Equation 2 can be rewritten as

$$\begin{aligned}E_f^{\text{int}} &= \frac{1}{2}(E_x^{\text{tot}} - n^{\text{GaN}} \mu^{\text{GaN}} - n^{\text{ZnO}} \mu^{\text{ZnO}} - \Delta n^{\text{Ga}} \mu^{\text{Ga}} \\ &\quad - \Delta n^{\text{Zn}} \mu^{\text{Zn}})/(ab)\end{aligned}\quad (4)$$

where  $\Delta n^{\text{Ga}} = n^{\text{Ga}} - n^{\text{N}}$  and  $\Delta n^{\text{Zn}} = n^{\text{Zn}} - n^{\text{O}}$  account for the deviation from the ideal bulk stoichiometry. However, the supercells considered in this study can all be represented in terms of integer numbers of ZnO and GaN pairs and hence the interfacial formation energies can be derived in terms of the chemical potentials of GaN and ZnO only:

$$E_f^{\text{int}} = \frac{1}{2}(E_x^{\text{tot}} - n^{\text{GaN}} \mu^{\text{GaN}} - n^{\text{ZnO}} \mu^{\text{ZnO}})/(ab) \quad (5)$$

This avoids having the formation energy be dependent on  $\mu^{\text{Ga}}$ ,  $\mu^{\text{N}}$ ,  $\mu^{\text{Zn}}$  and  $\mu^{\text{O}}$ , the precise values of which are unknown. However, the polarity of both GaN and ZnO means that the two interfaces in the supercells will be different and therefore the interfacial formation energies determined using Equation 5 will correspond to an averaged formation energy for the two different interfaces. It is therefore impossible to derive absolute interfacial formation energies using this approach. However, at least the relative stability of the various interfaces can be determined by keeping one of the two interfaces constant in all calculations, which in turn is only possible for supercells containing crystal slabs of the same orientation. Hence, two sets of relative interfacial stabilities will be reported in this study—one involving interfacial bonds between the Zn-face of the ZnO slab and the N-face of the GaN slab (Zn–N interfaces) and another one involving interfacial bonds between the O-face of the ZnO slab and the Ga-face of the GaN slab (Ga–O interfaces).

As only relative formation energies can be determined, the factor of  $1/2$  in Equation 5 above has to be removed since energy *differences* between the various interfaces are being considered. In other words, by subtracting the formation energy of one supercell from the formation energy of another supercell containing the same reference interface, the reference interface is effectively removed and hence the relative stability of the interfaces of interest can be obtained. This can be expressed as:

$$\Delta E_f^{\text{int}} = E_f^{\text{SL}_1} - E_f^{\text{SL}_2} \quad (6)$$

where  $E_f^{\text{SL}_x}$  is the formation energy of the two interfaces contained in supercell  $x$ , which is given by:

$$E_f^{\text{SL}_x} = (E_x^{\text{tot}} - n_x^{\text{GaN}} \mu^{\text{GaN}} - n_x^{\text{ZnO}} \mu^{\text{ZnO}})/(ab) \quad (7)$$

where  $E_x^{\text{tot}}$  is the calculated total energy of supercell  $x$ , containing  $n_x^{\text{GaN}}$  GaN units and  $n_x^{\text{ZnO}}$  ZnO units.

### 2.3. The valence band offset

The determination of the valence-band offset across the interface between two semiconductor materials involves lining up the band structures of the two materials. Hence, the band structures of the two semiconductors have to be determined with respect to some reference level, which is generally chosen to be their macroscopic average electrostatic potential,  $\bar{V}$ . The valence band offset is then determined by aligning the macroscopic average electrostatic potentials of the two semiconductors.

For the purpose of determining the valence band offset between two semiconductor slabs, only the variation of the electrostatic potential perpendicular to the interfacial plane is of interest. The other two coordinates can be removed by averaging in planes parallel to the interface:

$$\bar{V}(z) = \frac{1}{S} \int_S V(x, y, z) dx dy, \quad (8)$$

where  $S$  is the area of the unit cell in the plane of the interface. This results in a one-dimensional function that still exhibits periodic variations in the direction perpendicular to the interface. The macroscopic average is then found by averaging  $\bar{V}(z)$  over a distance corresponding to one period:

$$\bar{\bar{V}}(z) = \frac{1}{a} \int_{z-a/2}^{z+a/2} \bar{V}(z') dz', \quad (9)$$

where  $a$  is the length of one period in the  $z$ -direction. However,  $\bar{V}$  cannot be determined on an absolute scale [24] and hence a common reference for the two macroscopic average electrostatic potentials,  $\bar{V}_A$  and  $\bar{V}_B$ , has to be found. In order to find that common reference,  $\bar{V}_A$  and  $\bar{V}_B$  have to be determined from a calculation involving both semiconductor slabs joined at the interface. This ensures that the electrostatic potentials of both materials are expressed with respect to the same reference and allows direct extraction of  $\Delta \bar{\bar{V}}_{\text{int}}$ , which is defined as the offset of the average electrostatic potential across the interface. The valence-band offset,  $\Delta E_v$ , can then be determined using

$$\Delta E_v = \Delta \bar{\bar{V}}_{\text{int}} + (E_v^A - \bar{V}_{\text{bulk}}^A) - (E_v^B - \bar{V}_{\text{bulk}}^B) \quad (10)$$

where  $E_v^A$  and  $E_v^B$  are the valence band maxima of semiconductor  $A$  and  $B$ , respectively. Note that  $E_v^A$ ,  $\bar{V}_{\text{bulk}}^A$ ,  $E_v^B$  and  $\bar{V}_{\text{bulk}}^B$  are all bulk properties, while  $\Delta \bar{\bar{V}}_{\text{int}}$  depends on the atomic structure of the interface. A

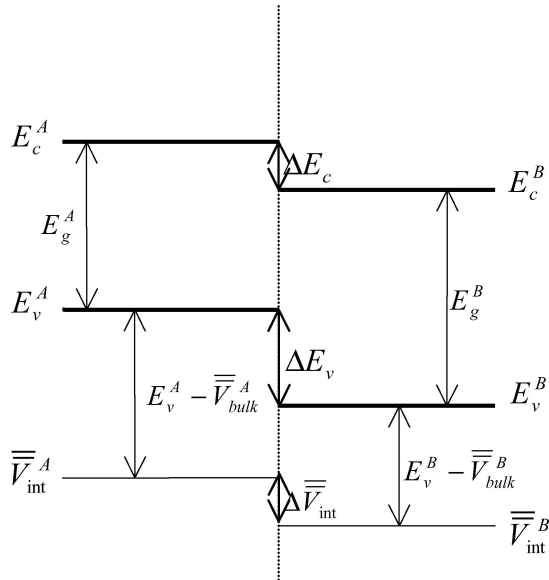


Figure 2 Schematic diagram of the band line-up at the interface between semiconductors A and B, exhibiting different band gaps,  $E_g^A$  and  $E_g^B$ .  $\bar{V}_{int}^A$  and  $\bar{V}_{int}^B$  are the macroscopic average electrostatic potentials of semiconductor slab A and B joined at the interface.  $E_c^A$  and  $E_c^B$  are the conduction band minima and  $\Delta E_c$  is the conduction band offset. Adapted from [24].

schematic diagram of the procedure used to determine the valence band offset is shown in Fig. 2.

In order to derive the macroscopic average electrostatic potentials of the two semiconductor slabs joined at the interface, it is necessary to find a 'bulk-like' region in each of the two semiconductor slabs, where the value of the macroscopic average electrostatic potential can be determined. In other words, a region of the semiconductor slabs has to be identified that is not significantly affected by the interface. It should be noted that the calculated valence-band offset can also be used to determine the conduction band offset, provided the band gaps of the two semiconductor materials joined at the interface is known.

The observed valence-band offset at a polar, heterovalent semiconductor interface is strongly dependent on the interfacial atomic configuration. Depending on the relative position of the charge-deficient and charge-rich bonds at the interface, interfacial dipoles of different orientations will be formed, as is indicated in Fig. 1. In particular, the dipoles at cation- and anion-compensated interfaces point in exactly opposite directions, which is why different band offsets are expected at the differently compensated interfaces. This dependence of the band offset on the atomic structure of the interface opens the possibility of controlled band offset engineering.

#### 2.4. Interfaces considered

In this study ideally stacked, compensated interfaces (involving one mixed interfacial layer only) between ZnO (0001) and GaN (0001), excluding interfaces involving cation-cation or anion-anion interfacial bonds, were considered. In addition to the cation- and anion-compensated Ga–O interfaces between a Ga-

terminated slab of GaN and an O-terminated slab of ZnO, shown in Fig. 1, the cation- and anion-compensated Zn–N interfaces between a N-terminated slab of GaN and a Zn-terminated slab of ZnO were considered. The supercells used to determine the relative stability of the various interfaces are depicted in Fig. 3.

Note that an averaged basal-plane lattice constant of the bulk ZnO and GaN cells has been used for all supercells considered in this study. However, all cell constants were allowed to relax in all calculations, which resulted in basal plane lattice constants ranging from 6.453 to 6.457 Å.

### 3. Computational details

The calculations described below are based on density functional theory using the PBE [25] exchange correlation functional. The wave functions were expanded using a plane-wave basis set up to an energy cut-off of 380 eV, which is found to reproduce the bulk lattice constants of ZnO and GaN to within 0.9% of the experimental values. The electron-ion interaction is described using ultrasoft pseudopotentials [26] and the d-electrons in Zn and Ga are modelled explicitly. Relaxation of the atomic structure is performed until forces on the atoms are less than 0.03 eV/Å. The Brillouin zones of all compensated supercells, containing four atoms in the interfacial plane and either 5 or 7 double layers (defined as a Ga–N or Zn–O pair of planes) of either semiconductor material parallel to the interface, are sampled using a  $4 \times 4 \times 1$  Monkhorst Pack [27]  $k$ -point grid. The Brillouin zone of the supercells containing the non-compensated interfaces, containing only one atom in the interfacial plane and between 3 and 9 double layers of both ZnO and GaN parallel to the interface, is sampled using a  $8 \times 8 \times n$   $k$ -point grid, where  $n$  varied depending on the length of the supercell. Hence the electronic structure of the supercell containing 3 double layers of either semiconductor material (henceforth referred to as a (3 + 3) supercell) was sampled using an  $8 \times 8 \times 2$   $k$ -point grid, while an  $8 \times 8 \times 1$   $k$ -point grid was used to sample the electronic structure of the larger supercells. The entire computational methodology is implemented in the CASTEP program [29].

### 4. Results and discussion

#### 4.1. Interfacial formation energies

The formation energies of the four supercells containing the different compensated interfaces considered, as well as the relative formation energies of the different interfaces are summarised in Table I.

The table shows that the cation-compensated interfaces are about 20 meV/unit cell more stable than the corresponding anion-compensated interfaces, irrespective of interfacial polarity. The fact that this pattern holds for interfaces of either polarity, suggests that the different stability of cation- and anion-compensated interfaces is not due to different bonding interactions at these interfaces, but rather due to another factor, such as the disturbance of the crystal periodicity by the introduction of the compensating anion, which appears to be

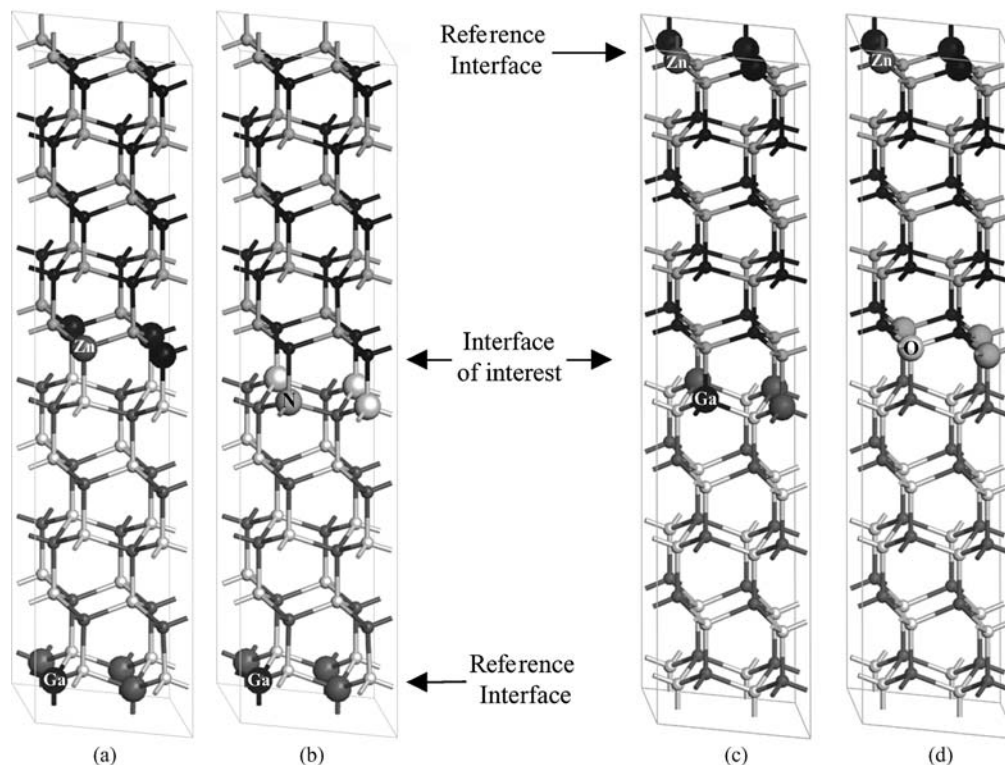


Figure 3 Supercells used to model (a) the Zn- and (b) N-compensated Ga-O interfaces and (c) the Ga- and (d) O-compensated Zn-N interfaces. The reference interface was chosen to be cation-compensated in all supercells, however, due to the polarity of the materials, the reference interface used in calculations of the Ga-O interface is different from the reference interface used in calculations of the Zn-N interface. The colour scheme is the same as in Fig. 1.

more pronounced than the corresponding perturbation to the crystal periodicity resulting from the insertion of the compensating cation.

It should be noted that (5 + 5) supercells were sufficient to determine the formation energy of the cation-compensated interfaces, while (7 + 7) supercells were needed to obtain converged results for the anion-compensated interfaces. The different convergence properties of cation- and anion-compensated interfaces can be explained in terms of the different directionality of the interfacial dipoles at these interfaces, mentioned in Section 2.3. Thus, irrespective of interfacial polarity, the interfacial dipole in cation-compensated interfaces points towards the GaN slab, while it points towards the ZnO slab in anion-compensated interfaces. Now, as the reference interface was chosen to be cation-compensated in all supercells, the interfacial dipoles of the two interfaces in the super-

cells containing the cation-compensated interfaces (of interest) both point towards the GaN slab, while they point towards different semiconductor slabs in supercells containing the anion-compensated interfaces—towards the GaN slab at the reference interface and towards the ZnO slab at the anion-compensated interface of interest. Hence in the supercells, containing the cation-compensated interfaces, no charge transfer between the interfaces is expected, while charge transfer between the interfaces is conceivable for supercells containing the anion-compensated interfaces. This charge transfer interaction is clearly dependent on the interfacial separation and hence explains the different observed convergence properties of cation- and anion-compensated interfaces.

In order to assess the effect of compensation on the interfacial stability, the formation energy of the non-compensated equivalent to the compensated Ga-O and Zn-N interfaces, depicted in Figs 3a and b, was determined. The formation energy of the (9 + 9) supercell containing the two non-compensated interfaces was determined to be 374 meV, which is more than double the formation energy of the supercells containing the corresponding compensated interfaces (see Table I). The actual formation energies of the non-compensated interfaces will be even larger, as the quoted result is not converged with respect to supercell-size perpendicular to the interfacial plane, as can be seen in Table II. The rapid increase in interfacial formation energy with increasing supercell size is due to the weakening of the attractive interaction between the electron-rich and the electron deficient interface with increasing interface-interface distance. This interaction is clearly spurious

TABLE I Relative stability of cation- and anion-compensated Ga-O and Zn-N interfaces.  $E_f^{SL}$  is the formation energy of the supercells containing the different interfaces, determined using Equation 7;  $\Delta E_{+/-}^{int}$  is the relative stability of the cation- and anion-compensated interfaces, which was determined using Equation 6. Note that the elements in brackets indicate the nature of the interfacial compensation

Interface	$E_f^{SL}$ (eV/unit cell)	$\Delta E_{+/-}^{int}$ [eV]
Zn-polarity ZnO		
Ga-O (Zn)	0.154	–
Ga-O (N)	0.175	0.021
O-polarity ZnO		
Zn-N (Ga)	0.155	–
Zn-N (O)	0.180	0.025

TABLE II Variation of the formation energy of a supercell containing two non-compensated interfaces, as a function of supercell size

Supercell size	$E_f^{SL}$ (eV/unit cell)	$\Delta E_f^{SL}$ (eV)
(3 + 3)	0.096	–
(5 + 5)	0.222	0.126
(7 + 7)	0.330	0.108
(9 + 9)	0.389	0.059

and the supercell size has to be increased until the calculated interfacial formation energies cease to exhibit a dependence on supercell size.

#### 4.2. Valence band off-sets

The valence band offsets (VBO) at the cation- and anion-compensated interfaces were determined using (5 + 5) supercells, having both interfaces either cation- or anion compensated. As was pointed out before, the two interfaces in these supercells are different. The VBO at these interfaces will nonetheless be very similar, since they mainly depend on the interfacial dipoles, which point towards the same semiconductor slab at equally compensated interfaces. A plot of the electrostatic potential along the  $z$ -axis of the supercell [0001] containing the cation-compensated Ga–O and Zn–n interfaces is shown in Fig. 4.

The band structure of appropriately strained bulk ZnO and GaN were aligned to the average electrostatic potential of the corresponding semiconductor slab in the supercell containing the interfaces, as described in Section 2.3 above, to yield the valence band offsets given in Table III.

The calculated valence band offsets correspond well to the experimentally found band offset of 0.8 eV [28].

TABLE III The valence band offsets at the cation- and anion-compensated interfaces

Interface	VBO (eV)
GaO(Zn)/ZnN(Ga)	1.0
GaO(N)/ZnN(O)	0.5

However, they are substantially smaller than the theoretical band offsets previously reported by Nakayama *et al.* [21], who found a VBO of 2.2 and 1.0 eV at the cation- and anion-compensated interface, respectively. The difference in the calculated band-offsets may well be due to the different methodologies used. In particular, Nakayama *et al.* treated the  $d$ -electrons of Zn as core electrons, while they were modelled explicitly in this study. In addition, Nakayama *et al.* employed the virtual crystal approximation, while the actual interfacial structure was considered in this study. However, in agreement with Nakayama *et al.* and experimental data [28], it was found that the band offsets at the cation- and the anion-compensated interface are of type 2 alignment with the valence band maximum and the conduction band minimum of ZnO lying below the valence band maximum and the conduction band minimum of GaN, respectively.

#### 5. Conclusions

Both the relative formation energies and the valence band offsets at lattice-matched interfaces between (0001) GaN and (0001) ZnO have been determined. It was found that compensated interfaces are more than twice as stable as non-compensated interfaces. In addition, cation compensated interfaces were determined to be about 20 meV/unit cell more stable than the

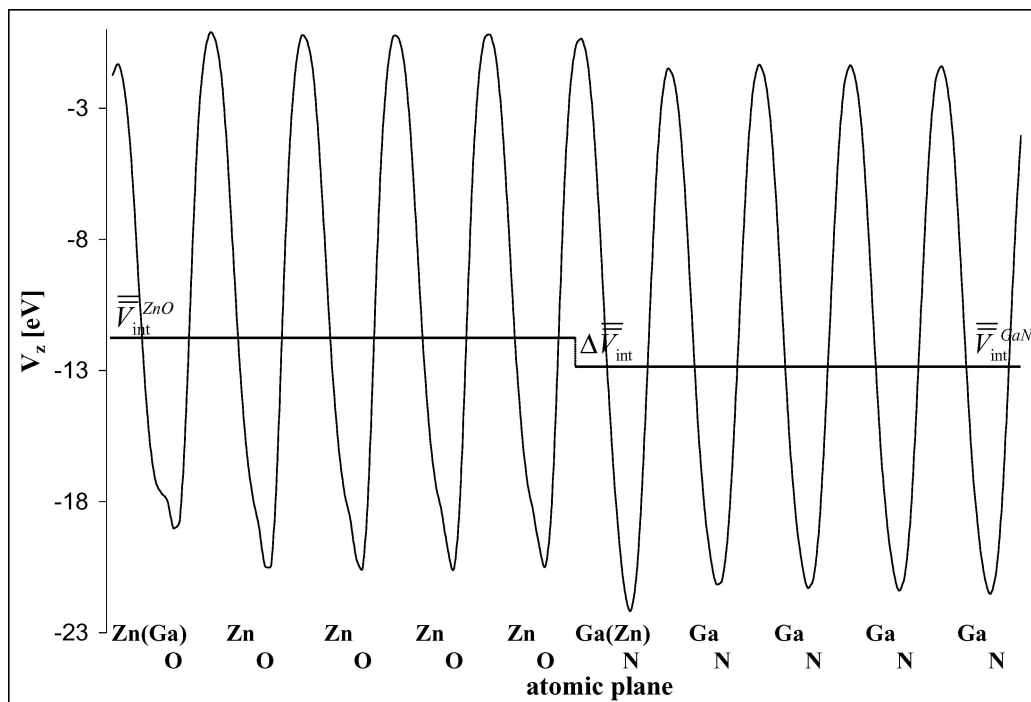


Figure 4 Variation of the average electrostatic potential in the supercell along [0001] normal to the cation-compensated interfaces. The macroscopic average electrostatic potential of ZnO,  $\bar{V}_{int}^{ZnO}$ , and GaN,  $\bar{V}_{int}^{GaN}$ , are indicated, as well as the change in electrostatic potential,  $\Delta \bar{V}_{int}$ , across the interfaces.

corresponding anion-compensated interfaces, irrespective of interfacial polarity. This energy difference is very small and hence the nature of the interfacial compensation will be largely dependant on the growth conditions employed. Type 2 valence band offsets of 1.0 and 0.5 eV were found at the cation- and anion-compensated interfaces, respectively. The effect of strain on the stability and the valence band offset of the ZnO–GaN interface is currently being investigated and will be reported in a separate communication.

### Acknowledgements

This work was supported by the EPSRC and the calculations were performed at the Cambridge Cranfield High Performance Computing Facility.

### References

1. S. NAKAMURA, *J. Cryst. Growth* **145** (1994) 911.
2. S. NAKAMURA, M. SENOH, S. NAGAHAMA, N. IWASA, T. YAMADA, T. MATSUSHITA, H. KIYOKU and Y. SUGIMOTO, *Appl. Phys. Lett.* **68** (1996) 2105.
3. C. KLIGSHIRN, *Physica Status Solidi B* **71** (1975) 547.
4. W. A. HARRISON, "Electronic Structure and the Properties of Solids" (Dover Publications, New York, 1989) p. 176, Table 7-3.
5. S. K. HONG, H. J. KO, Y. CHEN, T. HANADA and T. YAO, *J. Vac. Sci. Techn. B* **18**(4) (2000) 2313.
6. D. C. LOOK, *Mater. Sci. Engng.* **B80** (2001) 383.
7. B. N. SVERDLOV, G. A. MARTIN, H. MORKOÇ and D. J. SMITH, *Appl. Phys. Lett.* **67**(14) (1995) 2063.
8. F. HAMDANI, A. BOTCHKAREV, W. KIM, H. MORKOÇ, M. YEADON, J. M. GIBSON, S.-C. Y. TSEN, D. J. SMITH, D. C. REYNOLDS, D. C. LOOK, K. EVANS, C. W. LITTON, W. C. MITCHEL and P. HEMENGER, *ibid.* **70** (1997) 467.
9. S. GU, R. ZHANG, J. SUN, L. ZHANG and T. F. KUECH, *MRS Int. J. Nitr. Semicond. Res.* **5S1** (2000) W3.15.
10. R. P. WANG, H. MUTO, Y. YAMADA and T. KUSUMORI, *Thin Solid Films* **411** (2002) 69.
11. F. HAMDANI, M. YEADON, DAVID J. SMITH, H. TANG, W. KIM, A. SALVADOR, A. E. BOTCHKAREV, J. M. GIBSON, A. Y. POLYAKOV, M. SKOWRONSKI and H. MOKOÇ, *J. Appl. Phys.* **83**(2) (1998) 983.
12. T. MATSUOKA, N. YOSHIMOTO, T. SASAKI and A. KATSUI, *J. Electr. Mater.* **21** (1992) 157.
13. Z. SITAR, M. J. PAISLEY, B. YAN and R. F. DAVIS, *Mater. Res. Soc. Symp. Proc.* **162** (1990) 537.
14. S. GU, R. ZHANG, J. SUN, L. ZHANG and T. F. KUECH, *MRS Int. J. Nitr. Semicond. Res.* **5S1** (2000) W3.15.
15. E. S. HELLMAN, *ibid.* **1** (1996) 16.
16. R. D. VISPUTE, V. TALYANSKY, S. CHOOPUN, R. P. SHARMA, T. VENKATESAN, M. HE, X. TANG, J. B. HALPERN, M. G. SPENCER, Y. X. LI, L. G. SALAMANCE-RIBA, A. A. ILIADIS and K. A. JONES, *Appl. Phys. Lett.* **73**(3) (1998) 348.
17. B. ZHAO, H. YANG, G. DU, G. MIAO, Y. ZHANG, Z. GO, T. YANG, J. WANG, W. LI, Y. MA, X. YANG, B. LIU, D. LIU and X. FANG, *J. Cryst. Growth* **258** (2003) 130.
18. H. KATO, M. SANO, K. MIYAMOTO and T. YAO, *J. Appl. Phys.* **92**(4) (2003) 1960.
19. Y. I. ALIVOV, J. E. VAN NOSTRAND, D. C. LOOK, M. V. CHUKICHEV and B. M. ATAIEV, *Appl. Phys. Lett.* **83**(14) (2003) 2943.
20. M. E. ABDELSALAM, P. N. BARLETT, J. J. BAUMBERG and S. COYLE, *Adv. Mater.* **16**(1) (2004) 87–90.
21. T. NAKAYAMA and M. MURAYAMA, *J. Cryst. Growth* **214** (2000) 299.
22. W. A. HARRISON, E. A. KRAUT, J. A. WALDROP and R. W. GRANT, *Phys. Rev B* **18**(8) (1978) 4402.
23. A. KLEY and J. NEUGEBAUER, *ibid.* **50**(12) (1994) 8616.
24. A. FRANCIOSI and C. G. VAN DE WALLE, *Surf. Sci. Rep.* **25** (1996) 34.
25. J. PERDEW, K. BURKE and M. ERNZERHOF, *Phys. Rev. Lett.* **77**(18) (1996) 3865.
26. D. VANDERBILT, *Phys. Rev. B* **41** (1990) 7892.
27. H. J. MONKHORST and J. D. PACK, *ibid.* **13** (1976) 5188.
28. S.-K. HONG, T. HANADA, H. MAKINO, H.-J. KO, Y. CHEN, A. TANAKA, H. SASAKI, S. SATO, D. IMAI, K. ARAKI and M. SHINOHARA, *J. Vac. Sci. Techn. B* **19**(4) (2001) 1429.
29. M. D. SEGALL, P. L. D. LINDAN, M. J. PROBERT, C. J. PICKARD, P. J. HASNIP, S. J. CLARK and M. C. PAYNE, *J. Phys.: Cond. Matter* **14**(11) (2002) 2717.

Received 29 July 2004  
and accepted 31 January 2005